

Converse magnetoelectric effect in three-phase composites of piezoceramic, metal cap, and magnet

Wai Yin Wong, Siu Wing Or,^{a)} and Helen Lai Wa Chan

Department of Applied Physics, The Hong Kong Polytechnic University, Hung Hom, Kowloon, Hong Kong

Yanmin Jia

Department of Applied Physics, The Hong Kong Polytechnic University, Hung Hom, Kowloon, Hong Kong and Shanghai Institute of Ceramics, Chinese Academy of Sciences, Shanghai 201800, China

Haosu Luo

Shanghai Institute of Ceramics, Chinese Academy of Sciences, Shanghai 201800, China

(Presented on 11 January 2007; received 31 October 2006; accepted 27 November 2006; published online 24 April 2007)

We report experimentally and theoretically the converse magnetoelectric (CME) effect in a three-phase piezoceramic-metal-cap-magnet composite made by sandwiching a thickness-polarized $\text{Pb}(\text{Zr}_x\text{Ti}_{1-x})\text{O}_3$ (PZT) disk between two truncated conical brass caps and two thickness-magnetized SmCo disks. The reported CME effect originates from the product of the converse piezoelectric effect in the PZT disk, the mechanical transformation/amplification effect in the brass caps, and the magnetic induction effect in the SmCo disks. The composite exhibits a large CME coefficient (α_B) in excess of 2 mG/V with a flat response in the broad frequency range of 0.1–100 kHz. The measured magnetic flux density shows an extremely linear relationship to the applied voltage with amplitude varying from 10 to 100 V over a wide range of detection distance of 0.7–6.5 mm. This electromechanically coupled effect enables applications of the composite in coil-free magnetic flux control devices, featuring smaller Joule heating loss, wider operational bandwidth, and greater property-tailorable flexibility compared to conventional electromagnet-based devices.

© 2007 American Institute of Physics. [DOI: [10.1063/1.2710214](https://doi.org/10.1063/1.2710214)]

I. INTRODUCTION

Magnetoelectric (ME) materials are a main class of multiferroic materials in which an applied magnetic field leads to an electric polarization response or, conversely, an applied electric field results in a magnetization response.¹ Importantly, the direct ME (DME) and converse ME (CME) effects can realize power-free magnetic field sensing devices and core-free magnetic flux control devices, respectively. In the past decades, a great deal of research efforts has been devoted to the DME effect, first in single-phase materials (e.g., Cr_2O_3),² then in two-phase magnetostrictive-piezoelectric composites,^{3,4} and lately in three-phase polymer-bonded magnetostrictive-piezoelectric composites.^{5,6}

However, few of reports have been made on the CME effect in the ME composites, especially when the effect is to be qualitatively described by the CME coefficient (α_B) defined by a change in magnetic flux density in response to an applied ac voltage (dB/dV).⁷ Following the idea of three-phase composites, we have developed a promising type of three-phase piezoceramic-metal-cap-magnet composite by bonding a thickness-polarized PZT disk between two specifically designed (nonmagnetic) brass caps and two thickness-magnetized SmCo disks. In this paper, we describe the structure and working principle of such a composite and report its CME effect at various applied ac voltages, frequencies, and detection distances.

II. STRUCTURE AND WORKING PRINCIPLE

Figure 1 illustrates the schematic diagram and photograph of the proposed piezoceramic-metal-cap-magnet composite. The composite consists of a disk-shaped piezoceramic PZT, two truncated conical brass caps, and two disk-shaped SmCo magnets arranged symmetrically along the thickness (or the z or z) direction and with their interfaces being bonded using an epoxy adhesive. The PZT disk, with a diameter ($2r_P$) of 13 mm, an electroded diameter ($2r_{Ps}$) of 9 mm, and a thickness (t_P) of 1 mm, was prepared using PKI552 powders and polarized using the two electroded surfaces normal to its thickness. The thickness and transverse piezoelectric strain coefficients (d_{33} and d_{31}) of the PZT disk were measured to be 540 and -230 pm/V, respectively. The two brass caps, each of 3 mm top-cavity diameter ($2r_{Cs}$), 9 mm bottom-cavity diameter ($2r_{Cb}$), and 0.6 mm cavity height (t_{Ch}), were made by die-punching a brass sheet with thickness (t_C) of 0.3 mm. The two SmCo disks were commercially supplied with a diameter ($2r_M$) of 8 mm, a thickness (t_M) of 2.6 mm, and a mass of 0.96 g. They were galvanized using nickel and their saturation magnetization (M_s) was known to be 875 kA/m. The north (N) and south (S) poles of the SmCo disks were normal to their main faces and also parallel to the thickness direction of the composite.

The working principle of our three-phase composite (Fig. 1) is essentially based on the product effect of the converse piezoelectricity of the PZT disk, the mechanical transformation/amplification of the brass caps, and the mag-

^{a)}Author to whom correspondence should be addressed; electronic mail: apswor@polyu.edu.hk

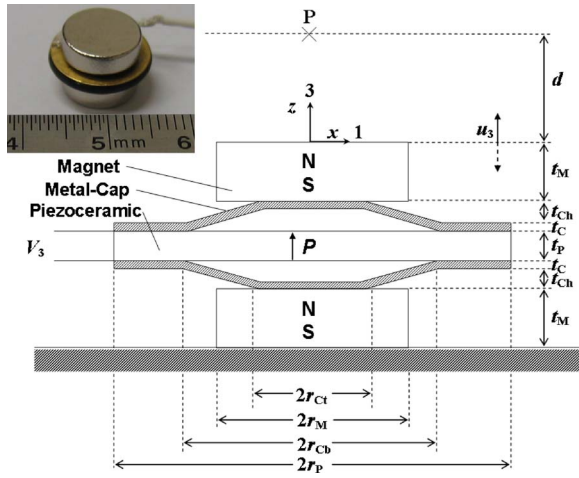


FIG. 1. Schematic diagram and photograph of our three-phase composite. The arrow P denotes the electric polarization direction.

netic induction of the SmCo disks. It is assumed that the composite is fixed at one end (i.e., the lower SmCo disk), while its other end (i.e., the upper SmCo disk) remains mechanically free. This produces dc magnetic flux lines along the thickness direction of the composite. If P is the detection point located at the z axis with a distance d from the surface center of the upper SmCo disk, the dc magnetic flux density at P is B_{3o} . In operation, applying an external ac voltage (V_3) to the input terminals of the composite produces an ac electric field across the thickness of the PZT disk (t_p), leading to both axial and radial motions of the disk. The piezoelectrically induced radial motion is subsequently transformed into flexural and rotational motions by the brass caps, resulting in an amplified motion parallel to the axial motion of the PZT disk. The combination of the axial and transformed/amplified axial motions in the cap-disk assembly displaces axially the upper SmCo disk towards/away from P with an ac displacement (u_3), giving rise to an ac magnetic flux density (B_3) superimposed on B_{3o} at P . It is noted that besides adjusting the properties of individual material phases as in the case of conventional ME composites,³⁻⁶ the properties of our composite can be tailored by altering the geometric parameters of the metal caps. In addition, while the upper magnet mainly contributes to B_3 , it is preferably to match that with the lower magnet in order to provide a symmetric magnetic prestress for preventing the whole composite structure from fracture especially during the expansion phases of oscillations.

For magnetic flux control device applications, we analyze the composite in Fig. 1 by limiting its operations at frequencies well below its fundamental shape resonance. Based on the current model for analyzing solid cylindrical magnets with uniform axial magnetization,⁸ the expression for the magnetic flux density produced by the composite along the z axis at the detection point P with a distance d can be derived as

$$B_3(z) = \frac{\mu_o M_s}{2} K,$$

$$K = \frac{z + t_M}{\sqrt{(z + t_M)^2 + r_M^2}} - \frac{z}{\sqrt{z^2 + r_M^2}} + \frac{z + L + 2t_M}{\sqrt{(z + L + 2t_M)^2 + r_M^2}} - \frac{z + L + t_M}{\sqrt{(z + L + t_M)^2 + r_M^2}}, \quad (1)$$

where $\mu_o (=4\pi \times 10^{-7} \text{ H/m})$ is the magnetic permeability of free space and $L (=2t_{Ch} + 2t_C + t_p)$ is the total thickness of the cap-disk assembly. The first two terms in Eq. (1) come from the upper magnet, while the latter two terms originate from the lower magnet. Hence, in the absence of V_3 , $B_3(z=d) = B_{3o}$ holds true; in the presence of V_3 , u_3 is induced, giving $B_3(z=d-u_3) = B_3$. For the cap-disk assembly, the d_{33} and d_{31} piezoelectric strain contributions from the piezoceramic disk are now combined and mediated by the mechanical transformation/amplification effect in the truncated conical metal caps to provide an effective piezoelectric strain coefficient d_{33}^{eff} for the composite. This yields⁹

$$d_{33}^{\text{eff}} = \beta(d_{33} - A d_{31}), \quad A = \frac{r_{Cb}(r_{Cb} - r_{Ct})}{t_{Ch}(t_p/2 + t_C)}, \quad (2)$$

where β is a constant related to the mass loading of the upper magnet and the magnetic prestress exerted by the upper and lower magnets ($=0.35$ in our design) and A is the transformation/amplification factor depending on the geometric parameters of the cap-disk assembly ($=28.125$ in our case). In material characterization, d_{33}^{eff} of the composite can be evaluated by

$$d_{33}^{\text{eff}} = \frac{t_p}{L} \frac{du_3}{dV_3}. \quad (3)$$

By differentiating $B_3(z=d-u_3) = B_3$ in Eq. (1) with respect to u_3 and then combining it with Eqs. (2) and (3), the CME coefficient (α_B) of the composite at P is obtained as

$$\alpha_B = \frac{dB_3}{dV_3} = \frac{dB_3}{du_3} \frac{du_3}{dV_3} = \mu_o M_s d_{33}^{\text{eff}} \frac{L}{2t_p} K',$$

$$K' = \left[\frac{1}{[(d + t_M)^2 + r_M^2]^{3/2}} - \frac{1}{(d^2 + r_M^2)^{3/2}} + \frac{1}{[(d + L + 2t_M)^2 + r_M^2]^{3/2}} - \frac{1}{[(d + L + t_M)^2 + r_M^2]^{3/2}} \right]. \quad (4)$$

From Eq. (4), it is clear that α_B of the composite mainly depends on M_s of the magnets, d_{33} and d_{31} of the piezoceramic disk, β of the magnet loading and magnetic prestress, and A of the cap-disk assembly, besides its geometric parameters and the detection distance d . Equations (1) and (4) indicate nonlinear relationships between B_{3o} and d and between α_B and d , respectively.

III. RESULTS AND DISCUSSION

Figure 2 shows the measured and predicted dc magnetic flux densities (B_{3o}) as a function of detection distance (d). The prediction is obtained by setting $B_3(z=d) = B_{3o}$ in Eq. (1) and found to agree well with the measurement. There is a

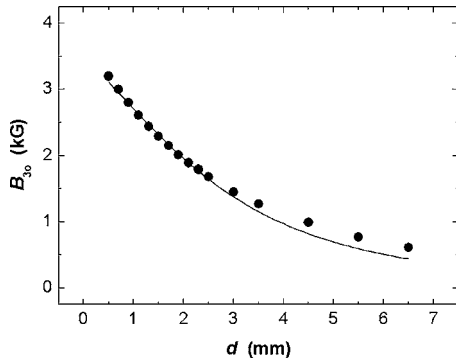


FIG. 2. Measured (dots) and predicted (line) dc magnetic flux densities (B_{3o}) as a function of detection distance (d).

gradual decrease in B_{3o} with increasing d . Nevertheless, the variation of B_{3o} with d remains quite linear for $d \leq 2.5$ mm.

Figure 3 plots the measured ac magnetic flux density (B_3) and displacement (u_3) as a function of applied ac voltage (V_3) in the V_3 range of 10–100 V peak at the frequency of 1 kHz for various detection distances (d) of 0.7–4.5 mm. For a given d , the two SmCo disks provide a certain value of B_{3o} , as shown in Fig. 2. By applying a V_3 to the composite, a u_3 is induced by the cap-disk assembly, due to the transformed/amplified converse piezoelectric effect, resulting in a change in B_{3o} and hence a B_3 . From the u_3 - V_3 plot, it is seen that u_3 increases linearly with V_3 . Based on the slope of the plot (i.e., the slope of the fitted dotted line), and according to Eq. (3), d_{33}^{eff} of the composite is determined to be 1196 pm/V. This experimental d_{33}^{eff} not only is much larger than the d_{33} (=540 pm/V) and d_{31} (=−230 pm/V) of the PZT disk but also coincides with the predicted d_{33}^{eff} of 1041 pm/V based on Eq. (2). Importantly, the linear relationship of u_3 - V_3 results in good linear responses of B_3 to V_3 in the entire V_3 range for all d . The inset shows a stable CME conversion from V_3 to B_3 and the high controllability nature of our composite.

Figure 4 illustrates the measured and predicted dependences of the CME coefficient (α_B) on the detection distance (d). The measured α_B values are obtained from the slopes of the B_3 - V_3 plots (i.e., the slopes of the fitted solid lines) at

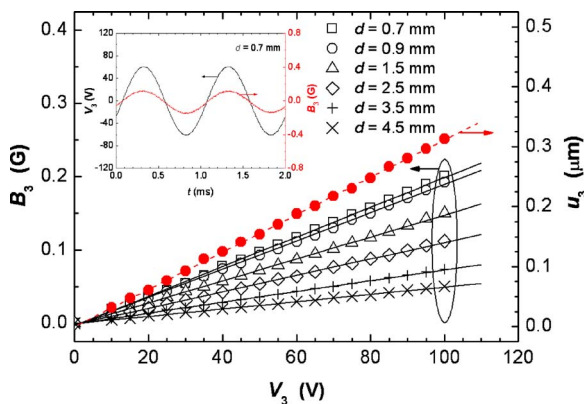


FIG. 3. Measured ac magnetic flux density (B_3) and displacement (u_3) as a function of applied ac voltage (V_3) at 1 kHz for various detection distances (d). The lines are the linearly fitted lines. The inset shows the wave forms of the measured B_3 due to an applied V_3 at 60 V peak with $d=0.7$ mm.

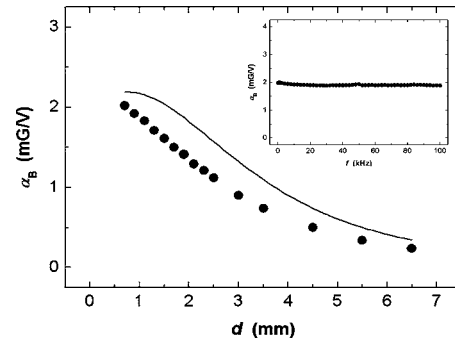


FIG. 4. Measured (dots) and predicted (line) dependences of the CME coefficient (α_B) on the detection distance (d). The inset shows the frequency (f) dependence of α_B at $d=0.7$ mm.

various d in Fig. 3, while the predicted α_B values are determined from Eq. (4). It is obvious that the measured α_B is in good agreement with the predicted α_B . Interestingly, the measured α_B , similar to the plot of B_{3o} - d in Fig. 2, decreases almost linearly for $d \leq 2.5$ mm. Beyond this 2.5 mm limit, it tends to deviate from the linear relationship and even to level off. The inset shows the frequency (f) dependence of α_B at $d=0.7$ mm. α_B has an essentially flat response in the measured f range of 0.1–100 kHz with no observable dispersion of the CME effect.

IV. CONCLUSION

The CME effect in the three-phase piezoceramic-metal-cap-magnet composite has been studied, both experimentally and theoretically. The results have demonstrated that the composite possesses a high α_B of >2 mG/V at $d < 0.7$ mm for f varying from 0.1 to 100 kHz, and a good linear relationship between B_3 and V_3 in the V_3 range of 10–100 V for d up to 6.5 mm. Comparing to the conventional electromagnet-based magnetic flux control devices, the composite is essentially based on the intrinsic CME effect to generate magnetic fluxes; it does not need any magnetic coil and thus has much lower Joule heating loss, broader operational bandwidth, and greater property-tailorable flexibility. These make the composite to be a promising material for direct realization of coil-free magnetic flux control devices.

ACKNOWLEDGMENTS

This work was supported by the Research Grants Council of the HKSAR Government under Grant No. PolyU 5122/05E.

- ¹L. D. Landau and E. Lifshitz, *Electrodynamics of Continuous Media* (Pergamon, Oxford, 1960).
- ²V. J. Folen, G. T. Rado, and E. W. Stalder, *Phys. Rev. Lett.* **6**, 607 (1961).
- ³J. Ryu, A. V. Carazo, K. Uchino, and H. Kim, *J. Electroceram.* **7**, 24 (2001).
- ⁴S. Dong, J. F. Li, and D. Viehland, *Appl. Phys. Lett.* **83**, 2265 (2003).
- ⁵S. W. Or and N. Cai, *Solid State Phenom.* **111**, 147 (2006).
- ⁶T. Li, S. W. Or, and H. L. W. Chan, *J. Magn. Magn. Mater.* **304**, e442 (2006).
- ⁷Y. Jia, S. W. Or, H. L. W. Chan, X. Zhao, and H. Luo, *Appl. Phys. Lett.* **88**, 242902 (2006).
- ⁸E. P. Furlani, *Permanent Magnet and Electromechanical Devices: Materials, Analysis, and Applications* (Academic, San Diego, 2001).
- ⁹P. Ochoa, M. Villegas, J. L. Pons, P. Leidinger, and J. F. Fernández, *J. Electroceram.* **14**, 221 (2005).

Journal of Applied Physics is copyrighted by the American Institute of Physics (AIP).
Redistribution of journal material is subject to the AIP online journal license and/or AIP
copyright. For more information, see <http://ojps.aip.org/japo/japcr/jsp>